

$C_6H_5 + NO \rightarrow C_6H_5NO$  as shown in Figure 2. This clearly demonstrates that the species formed by 193-nm excitation is phenyl radical.

The broad absorption spectra at 0 ns in Figures 1 and 2 are reasonably assigned to vibrationally highly excited, "hot" phenyl radicals. Its monotonous absorption can be interpreted primarily as a tail of the allowed transition corresponding to the  $S_3^{**}(E_{1u}) \leftarrow S_0^{**}$  of hot benzene. The absorptions of such hot molecules have already been observed in benzene and its derivatives: benzene,<sup>8</sup> toluene,<sup>10,11</sup> and hexafluorobenzene.<sup>12</sup> The available energy  $E_{avl}$  of the hot phenyl radical formed is calculated to be 221 kJ/mol.<sup>13</sup> A recent molecular beam photodissociation study has shown that chlorobenzene dissociates at 193 nm to produce vibrationally hot phenyl radicals with an average translational energy of 52 kJ/mol.<sup>15</sup> Assuming a negligible contribution of energy redistribution to rotational energy, we can estimate that the average vibrational energy in phenyl radical is about 169 kJ/mol. This energy corresponds to 1400 K in the vibrational temperature. The hot phenyl radicals are relaxed by collisions with foreign gases, as can be seen from Figure 1. For example, the fast decay in the absorption time profile at 230 nm is explained in terms of collisional cooling.<sup>7,8,10,12</sup> Consequently, an absorption spectrum at 100 ns in Figure 1 which has a band maximum around 245 nm is assigned to the relaxed phenyl radical.

The relaxed absorption spectrum is in good agreement with the results by pulse-radiolysis studies in solution.<sup>4,5</sup> The spectrum is distinctly different from that of cyclohexadienyl radical<sup>16</sup> or  $\pi$ -complex with halogen atom.<sup>17,18</sup> Although the observed spectra in Figure 1 is close to the spectrum of biphenyl which has a band maximum at 235 nm, a possibility of biphenyl formation within our time scale ( $\leq 150$  ns) is completely neglected for the following reasons: (1) In the presence of 800 torr of propane, we observed the same transient. Under such conditions, it is known that the final product is benzene, but not biphenyl, in steady-state photochemical studies.<sup>9</sup> (2) On the basis of the known rate constant of  $10^{13.0} \exp(-10 \text{ kcal}/RT) \text{ cm}^3 \text{ mol}^{-1} \text{ s}^{-1}$  for the reaction  $C_6H_5Br + C_6H_5 \rightarrow C_6H_5C_6H_5 + Br$ ,<sup>19</sup> biphenyl formation at 100 ns in the present system is estimated to be negligibly small. (3) A linear relation between the transient absorbance at 100 ns vs. the excitation intensity was obtained. If phenyl radicals would recombine themselves to form biphenyl, the absorbance should be proportional to the square of the excitation intensity. Multiphoton processes are also disregarded from this result.

Trapping of nitrosobenzene in the presence of nitrogen monoxide is a simple method to detect phenyl radical and to estimate the quantum yield, because nitrosobenzene has the characteristic absorption with a relatively large molar extinction coefficient ( $12000 \text{ M}^{-1} \text{ cm}^{-1}$  at 270 nm).<sup>20</sup> Formation of phenyl radical was observed with good yields in the photolysis of bromobenzene, iodobenzene, and pentafluorochlorobenzene. It is interesting to note, however, that the yields of phenyl radical are very low in the case of pentafluorobenzene,  $\alpha, \alpha, \alpha$ -trifluorotoluene, and also benzene,<sup>8</sup> although the photon energy is high enough to form phenyl-type radicals. The details will be published elsewhere.

## Nitric Oxide Adduct of the Binuclear Iron Center in Deoxyhemerythrin from *Phascolopsis gouldii*. Analogue of a Putative Intermediate in the Oxygenation Reaction

Judith M. Nocek and Donald M. Kurtz, Jr.\*

Department of Chemistry, Iowa State University  
Ames, Iowa 50011

J. Timothy Sage and Peter G. Debrunner

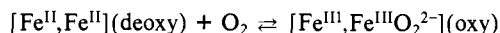
Department of Physics, University of Illinois  
at Urbana-Champaign, Urbana, Illinois 61801

Michael J. Maroney and Lawrence Que, Jr.

Department of Chemistry, University of Minnesota  
Minneapolis, Minnesota 55455

Received November 1, 1984

Hemerythrin (Hr) is a non-heme protein containing a binuclear iron site which reversibly binds molecular oxygen in several marine invertebrates.<sup>1</sup> A large body of physical and chemical evidence indicates that an appropriate formulation for the oxygenation reaction is



However, X-ray crystallography<sup>2</sup> indicates that dioxygen has direct access to only one of the two iron atoms. Thus, if the formal oxidation state changes shown above are correct, one could postulate the existence of an intermediate between deoxy- and oxyHr, which would be formulated as  $[Fe^{II}, Fe^{III}O_2^-]$ . Such an intermediate has never been detected. However, its transient existence does not seem unreasonable in view of the fact that the two high-spin irons in deoxyHr have usually been described as magnetically uncoupled or nearly so, presumably due to lack of an appropriate bridging ligand. The two high spin irons in oxyHr, on the other hand, are antiferromagnetically coupled through a  $\mu$ -oxo bridge ( $J \sim -75 \text{ cm}^{-1}$ ).<sup>3,4</sup>

We report that a nitric oxide adduct of deoxyHr (deoxyNO) from *Phascolopsis gouldii* can be prepared, whose physical and chemical properties are consistent with its formulation as  $[Fe^{II}, Fe^{III}NO^-]$ . Thus, deoxyNO can be viewed as an analogue of the putative intermediate in the oxygenation reaction. The most pertinent feature of the NO adduct is that the irons are magnetically coupled.

Gradual injection over the course of  $\sim 5$  min of a 1.5–4-fold molar excess of gaseous NO to an anaerobic solution of deoxyHr<sup>5</sup> at room temperature results in development of a pine-green color. The optical spectra are shown in Figure 1. Features in the spectrum of deoxyNO at 408 ( $\sim 1000 \text{ M}^{-1} \text{ cm}^{-1}$ ), 500 ( $\sim 600 \text{ M}^{-1} \text{ cm}^{-1}$ ), and 600 nm ( $\sim 400 \text{ M}^{-1} \text{ cm}^{-1}$ ) are quite different from those of any other derivative of Hr.<sup>1</sup> A sample of deoxyHr (EPR silent) frozen  $\sim 9$  min after injection of NO elicits an EPR spectrum (Figure 2, top) which is different from those of Hr in oxy and met ( $[Fe^{III}, Fe^{III}]$ ,  $S = 0$ , EPR silent) or semi-met ( $[Fe^{II}, Fe^{III}]$ ,  $S = 1/2$ ,  $g_{av} \sim 1.84$ ) oxidation levels.<sup>1</sup> Double integration of the rather broad, axial signal in Figure 2 vs. a  $CuSO_4$  standard yields 0.9 spins/ $2Fe$ .<sup>7</sup> The deoxyNO EPR spectrum disappears at  $\sim 34$

(10) Hippler, H.; Troe, J.; Wendelken, H. *J. Chem. Phys.* **1983**, *78*, 5351–5357. Astholz, D. C.; Brouwer, L.; Troe, J. *Ber. Bunsenges. Phys. Chem.* **1981**, *85*, 559–564.

(11) Ikeda, N.; Nakashima, N.; Yoshihara, K., unpublished results.

(12) Ichimura, T.; Mori, Y.; Nakashima, N.; Yoshihara, K. *Chem. Phys. Lett.* **1984**, *104*, 533–537.

(13) The available energy is calculated by the following equation.  $E_{avl} = h\nu(193 \text{ nm}) + E_{int}(300 \text{ K}) - D_0 = 221 \text{ kJ/mol}$ , where  $E_{int}$  is the internal energy of the parent molecule and  $D_0$  is the dissociation energy of the C–Cl bond of chlorobenzene (406 kJ/mol).<sup>14</sup>

(14) "Handbook of Chemistry and Physics"; Weast, R. C.; CRC Press: Cleveland, 1978; p F247.

(15) Freedman, A.; Yang, S. C.; Kawasaki, M.; Bersohn, R. *J. Chem. Phys.* **1980**, *72*, 1028–1033.

(16) Shida, T.; Hanazaki, I. *Bull. Chem. Soc. Jpn.* **1969**, *43*, 646–651.

(17) Strong, R. L.; Rand, S. J.; Britt, J. A. *J. Am. Chem. Soc.* **1960**, *82*, 5053–5057.

(18) Yamamoto, N.; Kajikawa, T.; Sato, H.; Tsubomura, H. *J. Am. Chem. Soc.* **1969**, *91*, 265–267.

(19) Fujii, N.; Asaba, T. *Nippon Kagaku Kaishi* **1977**, 599–605.

(20) Tanaka, J. *Nippon Kagaku Zasshi* **1958**, *79*, 1114–1120.

(1) (a) Wilkins, R. G.; Harrington, P. C. *Adv. Inorg. Biochem.* **1983**, *5*, 51–85. (b) Klotz, I. M.; Kurtz, D. M., Jr. *Acc. Chem. Res.* **1984**, *17*, 16–22. (c) Sanders-Loehr, J.; Loehr, T. M. *Adv. Inorg. Biochem.* **1979**, *1*, 235–256.

(2) (a) Stenkamp, R. E.; Sieker, L. C.; Jensen, L. H. *J. Am. Chem. Soc.* **1984**, *106*, 618–622. (b) Stenkamp, R. E.; Sieker, L. C.; Jensen, L. H.; McCallum, J. D.; Sanders-Loehr, J. *Proc. Natl. Acad. Sci. U.S.A.* **1985**, *82*, 713–716.

(3) York, J. L.; Bearden, A. J. *Biochemistry* **1970**, *9*, 4549–4954.

(4) Dawson, J. W.; Gray, H. B.; Hoening, H. E.; Rossman, G. R.; Schredder, J. M.; Wang, R. H. *Biochemistry* **1972**, *11*, 461–465.

(5) DeoxyHr was prepared by anaerobic dialysis of oxyHr<sup>6</sup> against  $\sim 10$  mM  $Na_2S_2O_4$  followed by anaerobic dialysis against 50 mM phosphate pH 6.5 to remove excess reagents. Hr concentrations are expressed as dimeric iron.

(6) Klotz, I. M.; Klotz, T. A.; Fiess, H. A. *Arch. Biochem. Biophys.* **1957**, *68*, 284–299.

(7) When this sample was incubated at 4 °C the EPR signal decreased to  $\sim 40\%$  of its original intensity after 2 h.

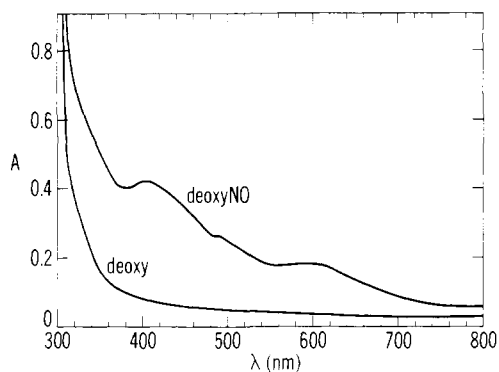


**Figure 1.** Absorption spectra of 0.54 mM deoxyHr and deoxyNO. DeoxyNO was prepared by addition of an  $\sim 4$ -fold molar excess over dimeric iron of gaseous NO in two aliquots to 1.88 mM deoxyHr in anaerobic 50 mM phosphate pH 6.5. The sample was then diluted to 0.54 mM. Cell path length = 1 cm.

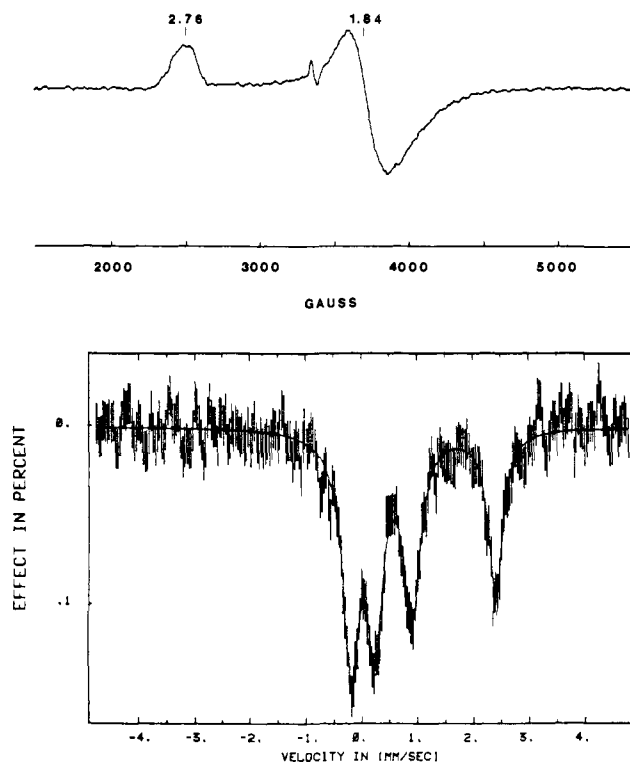


**Figure 2.** (Top) X-band EPR spectrum of 0.79 mM deoxyHr in 50 mM phosphate pH 6.5 frozen  $\sim 9$  min after addition of a 1.4-fold molar excess of gaseous NO. Spectral conditions: temperature, 4.1 K; frequency, 9.569 GHz; power, 40  $\mu$ W; modulation, 40 G at 100 kHz; receiver gain,  $8.0 \times 10^4$ ; time constant, 0.2 s. (Bottom)  $^{57}\text{Fe}$  Mössbauer spectrum recorded at 100 K of a portion of the same sample used to obtain the EPR spectrum. The solid curve represents a simulation assuming four Lorentzian components. Parameters are listed in the text.

K, a temperature dependence very similar to that of the semi-met EPR spectrum.<sup>1</sup>

Anaerobic addition of excess  $\text{N}_3^-$  or  $\text{CNO}^-$  to a solution of deoxyNO results in immediate bleaching of the pine-green color and disappearance of the EPR signal. Excess  $\text{Cl}^-$ ,  $\text{SCN}^-$ ,  $\text{CN}^-$ , or  $\text{ClO}_4^-$ , in contrast, has no detectable effect. This anion specificity is that observed for the bleaching of the oxyHr color.<sup>8</sup> Thus, the NO reaction is reversible and exhibits anion specificity similar to that of the deoxygenation reaction. That these anions may bind to the iron site in deoxyHr is indicated by changes in the paramagnetic  $^1\text{H}$  NMR spectra of deoxyHr in the absence and presence of  $\text{N}_3^-$  (Figure 3). DeoxyHr exhibits paramagnetic

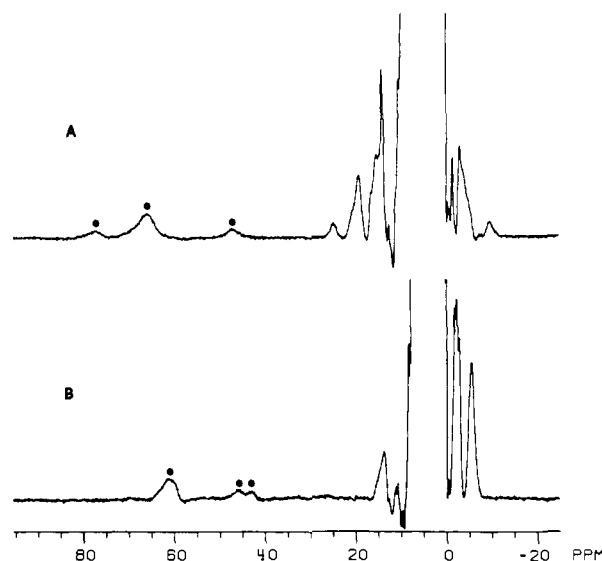


**Figure 3.**  $^1\text{H}$  NMR, 300 MHz, at 45  $^\circ\text{C}$  in 50 mM phosphate pH 7.5: (A) 3 mM deoxyHr plus a 30-fold molar excess of  $\text{NaN}_3$ , (B) 3 mM deoxyHr sample prior to addition of  $\text{NaN}_3$ . A  $\bullet$  denotes a solvent-exchangeable resonance.

resonances assignable to histidine  $\text{NH}$ 's.<sup>9</sup> The positions of these resonances are dramatically shifted upon addition of  $\text{N}_3^-$ . Thus, the bleaching of the deoxyNO (and oxyHr) color is due to an effect of  $\text{N}_3^-$  on the iron site.

An  $^{57}\text{Fe}$  Mössbauer spectrum was obtained of a portion of the sample used for the EPR spectrum. The Mössbauer spectrum (Figure 2, bottom) consists of four components of approximately equal widths and intensities at 100 K. Pairing the outermost components gives a quadrupole splitting (isomer shift) of 2.64 (1.23) mm/s. These values are characteristic of high-spin Fe(II) and are near those of deoxyHr (2.81 (1.19) mm/s at 77 K).<sup>11</sup> The corresponding values of the remaining inner pair of lines in the deoxyNO spectrum of 0.65 (0.68) mm/s are unique for Mössbauer spectra of Hr. However, these parameters are quite close to those of  $[\text{Fe}(5\text{-Cl-salen})\text{NO}]$  (0.58 (0.65) mm/s at 77 K), which has been characterized as a  $\{\text{FeNO}\}^7$   $S = 3/2$  system, as have several other non-heme ferrous nitrosyls with similar isomer shifts.<sup>12-14</sup> At 4.2 K all four components in the Mössbauer spectrum of deoxyNO broaden considerably (unlike deoxyHr) indicating that both iron atoms contribute to the paramagnetic center. These data are consistent with a description of the iron site in deoxyNO as  $[\text{Fe}(\text{II}) (S = 2), \{\text{FeNO}\}^7 (S = 3/2)]$ . Several mononuclear non-heme ferrous nitrosyls are known to give a characteristic axial or near axial  $S = 3/2$  type EPR spectrum with  $g_\perp \sim 4.0$  and  $g_\parallel \sim 2.0$ .<sup>13</sup> These values are quite different from those of Figure 2 for deoxyNO ( $g_\parallel = 2.76$ ,  $g_\perp = 1.84$ ). The discrepancy can be explained as due to antiferromagnetic coupling of the Fe(II) ( $S' = 2$ ) and  $\{\text{FeNO}\}^7$  ( $S = 3/2$ ) leading to a ground state  $S_{\text{eff}} = 1/2$ .<sup>16</sup> We are unaware of synthetic models where this type of coupling

(9) Recently paramagnetic  $^1\text{H}$  NMR spectra of metHr and semi-metHr have been obtained.<sup>10</sup>

(10) Maroney, M. J.; Lauffer, R. B.; Que, L., Jr.; Kurtz, D. M., Jr. *J. Am. Chem. Soc.* **1984**, *106*, 6445-6446.

(11) Garbett, K.; Johnson, C. E.; Klotz, I. M.; Okamura, M. Y.; Williams, R. J. P. *Arch. Biochem. Biophys.* **1971**, *142*, 574-583.

(12) Wells, F. V.; McCann, S. W.; Wickman, H. H.; Kessel, S. L.; Hendrickson, D. N.; Feltham, R. D. *Inorg. Chem.* **1982**, *21*, 2306-2311. 5-Cl-salen = ethylenebis(5-chlorosalicylideneamine).

(13) Arciero, D. M.; Lipscomb, J. D.; Hunyh, B. H.; Kent, T. A.; Münch, E. *J. Biol. Chem.* **1983**, *258*, 14981-14991.

(14) The  $\{\text{FeNO}\}^7$  notation follows that of Enemark and Feltham<sup>15</sup> for ferrous nitrosyls.

(15) Enemark, J. H.; Feltham, R. D. *Coord. Chem. Rev.* **1974**, *13*, 339-406.

(16) Similarly the EPR silent NO adduct of semi-metHr<sup>17</sup> can be described as antiferromagnetically coupled Fe(III) ( $S' = 5/2$ ) and  $\{\text{FeNO}\}^7$  ( $S = 3/2$ ) giving an  $S_{\text{eff}} = 1$  ground state. Integer spin systems are usually unobservable by EPR.

(8) Bradić, Z.; Conrad, R.; Wilkins, R. G. *J. Biol. Chem.* **1977**, *252*, 6069-6075.

occurs. On this basis a unique EPR spectrum is not surprising.<sup>18</sup>

Finally, we note that  $\{\text{FeNO}\}^7$  complexes having a bent FeNO geometry are often formulated as  $\text{Fe}^{\text{III}}\text{NO}^-$ .<sup>19</sup> On the basis of crystallographic results<sup>2</sup> for binding of  $\text{N}_3^-$  and  $\text{O}_2$  in metHr and oxyHr, respectively, a bent FeNO geometry is quite likely for deoxyNO. Thus,  $[\text{Fe}^{\text{II}}, \text{Fe}^{\text{III}}\text{NO}^-]$  would seem to be a reasonable formalism for the iron site. If deoxyNO represents an analogue of the proposed intermediate,  $[\text{Fe}^{\text{II}}, \text{Fe}^{\text{III}}\text{O}_2^-]$ , then our data suggest either that the iron atoms in deoxyHr are antiferromagnetically coupled (presumably through one or more bridging ligands) or that the originally uncoupled iron atoms in deoxyHr become coupled after binding of  $\text{O}_2$  to the exposed iron but prior to formal oxidation of the second iron. An EPR signature exists which could distinguish between these possibilities during earlier stages of the deoxyHr plus NO reaction, namely, the  $S = 3/2$  type with  $g \sim 4.0$  and 2.0.

**Note Added in Proof.** Recently, Reem and Solomon (*J. Am. Chem. Soc.* 1984, 106, 8323-8325) have presented evidence of weak antiferromagnetic exchange coupling ( $-J \sim 13 \text{ cm}^{-1}$ ) for the iron site in deoxyHr.

**Acknowledgment.** This work has been supported by the National Institutes of Health (D.M.K. GM 33157; P.G.D., GM 16406) and the National Science Foundation (L.Q. PCM-8314935). L.Q. is an Alfred P. Sloan Research Fellow and the recipient of a Research Career Development Award from the National Institutes of Health.

Registry No.  $\text{N}_3^-$ , 14343-69-2;  $\text{CNO}^-$ , 661-20-1; Fe, 7439-89-6.

(17) Nocek, J. M.; Kurtz, D. M., Jr.; Pickering, R. A.; Doyle, M. P. *J. Biol. Chem.* 1984, 259, 12334-12338.

(18) A model calculation assuming isotropic exchange  $\tilde{J}\tilde{S}\tilde{S}'$  between spins  $S = 3/2$  and  $S' = 2$  and including zero-field splitting for both sites allows one to produce a lowest doublet with effective  $g$  values close to the measured ones.

(19) McCleverty, J. A. *Chem. Rev.* 1979, 79, 53-76.

## Electronic Structure of a Metalated Doubly Bonded Group 15 Complex<sup>†</sup>

Kimberly A. Schugart and Richard F. Fenske\*

Department of Chemistry  
University of Wisconsin—Madison  
Madison, Wisconsin 53706

Received October 1, 1984

The unusual linkage of one or more transition-metal moieties to two doubly bonded group 15 atoms places such compounds among the structural exotica of inorganic complexes. A recent flurry of synthetic activity in this area has generated a wealth of these complexes<sup>1</sup> whose modes of bonding have far exceeded early workers' expectations.<sup>2</sup> Figure 1 illustrates some metal coordination modes thus far encountered, and Table I gives a partial listing of compounds whose structures have been verified by X-ray crystallography. Figure 1 schematically depicts two possible modes of coordination for transition-metal moieties to doubly bonded group 15 elements. Structures A and C involve end-on coordination alone while B and D exhibit simultaneous end-on and side-on coordination. Side-on coordination has been interpreted

<sup>†</sup> In this paper the periodic group notation is in accord with recent actions by IUPAC and ACS nomenclature committees. A and B notation is eliminated because of wide confusion. Groups IA and IIA become groups 1 and 2. The d-transition elements comprise groups 3 through 12, and the p-block elements comprise groups 13 through 18. (Note that the former Roman number designation is preserved in the last digit of the new numbering: e.g., III  $\rightarrow$  3 and 13.)

(1) For a recent review of the synthetic progress in this area, see: Cowley, A. H. *Polyhedron* 1984, 3, 389-432.

(2) Purcell, K. F.; Kotz, J. C. "Inorganic Chemistry"; W. B. Saunders: Philadelphia, 1977; Chapter 6, p 318.

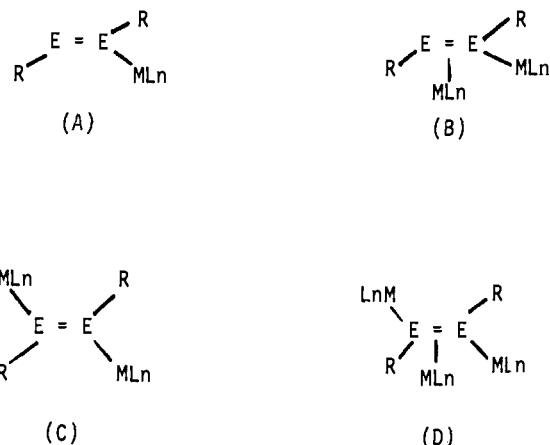


Figure 1. Illustrations of some encountered coordination modes for transition-metal moieties to two doubly bonded group 15 elements.

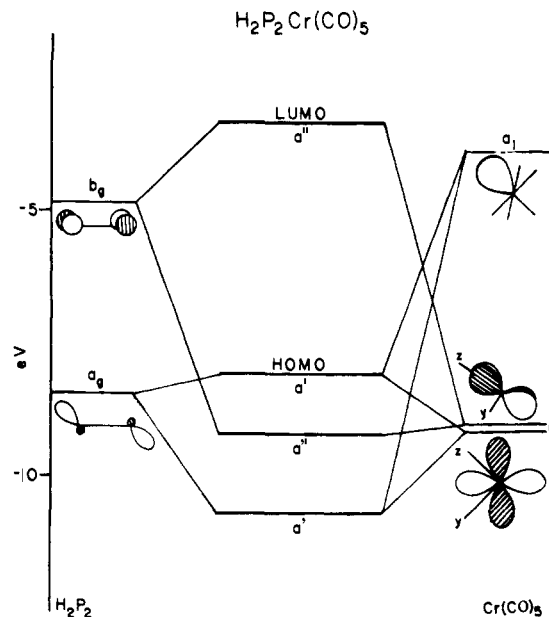


Figure 2. Molecular orbital scheme for  $\text{H}_2\text{P}_2\text{Cr}(\text{CO})_5$ . Only molecular orbitals containing interactions of the  $\text{H}_2\text{P}_2$  fragment and the  $\text{Cr}(\text{CO})_5$  moiety are depicted.

Table I

complex	type of bond (as shown in Figure 1)	ref
$(2,4,6\text{-}t\text{-Bu}_3\text{C}_6\text{H}_2)_2\text{P}_2\text{Fe}(\text{CO})_4$	A	3
$[\text{CH}(\text{SiMe}_3)_2]_2\text{P}_2\text{Cr}(\text{CO})_5$	A	4
$(2,4,6\text{-}t\text{-Bu}_3\text{C}_6\text{H}_2\text{O}_2)_2\text{P}_2[\mu\text{-Fe}(\text{CO})_4]\text{Fe}(\text{CO})_4$	B	5
$\text{H}_2\text{N}_2[\text{Cr}(\text{CO})_5]$	C	5
$[\text{CH}(\text{SiMe}_3)_2]_2\text{P}_2[\text{Fe}(\text{CO})_4]^2$	C	6
$(\text{C}_6\text{H}_5)_2\text{As}_2[\mu\text{-Cr}(\text{CO})_5(\text{Cr}(\text{CO})_3)]_2$	D	10

as a  $\pi$  interaction between metal and ligand orbitals, while end-on bonding has been construed as a purely  $\sigma$  interaction.<sup>3-7</sup> To ascertain the validity of these concepts, we have undertaken theoretical studies of the various modes of coordination. In this

(3) Cowley, A. H.; Kilduff, J. E.; Lasch, J. G.; Norman, N. C.; Pakulski, M.; Ando, F.; Wright, T. C. *J. Am. Chem. Soc.* 1983, 105, 7751-7752.

(4) Flynn, K. M.; Hope, H.; Murray, B. D.; Olmstead, M. M.; Power, P. P. *J. Am. Chem. Soc.* 1983, 105, 7750-7751.

(5) Huttner, G.; Gartzke, W.; Allinger, K. *J. Organomet. Chem.* 1975, 91, 47-56.

(6) Flynn, K. M.; Olmstead, M. M.; Power, P. P. *J. Am. Chem. Soc.* 1983, 105, 2085-2086.

(7) Cowley, A. H.; Kilduff, J. E.; Lasch, J. G.; Norman, N. C.; Pakulski, M.; Ando, F.; Wright, T. C. *Organometallics* 1984, 3, 1044-1050.